Printed Millimeter-Wave Reflectarrays

Dietmar PILZ*
Wolfgang MENZEL**

* now with DaimlerChrysler Aerospace, D-89070 Ulm, Germany
** Microwave Techniques, University of Ulm, D-89069 Ulm, Germany

Abstract

Periodic and quasi-periodic structures printed on a dielectric substrate can be employed to control reflection and transmission properties of incident waves as a function of structure geometry. This can be done mostly independently for both polarizations. These structures thus allow the realization of different kinds of filters and polarizers. Local variation of the element geometry on a substrate with backside metallization – resulting in respective variations of the reflection phase angle - can be employed to design printed reflectarray antennas. Including the dual polarization properties of such antennas, dual function or dual frequency antennas can be built, or these properties can be exploited for the realization of compact, low-profile folded reflector antennas. Examples for a number of antennas are presented, including dual radiation characteristics, dual frequency operation, and very compact, low loss folded reflector antennas.

Key words: Reflector antennas, Reflectarrays, Planar antennas, Spectral domain method

Antennes utilisant des réflecteurs à motifs imprimés

Résumé

Les structures périodiques et quasi-périodiques, imprimées sur un substrat diélectrique peuvent être employées pour contrôler les propriétés de réflexion et de transmission des ondes incidentes en fonction de la structure géométrique. Ceci peut être réalisé pratiquement indépendamment pour les deux polarisations. Ainsi des structures périodiques permettent la réalisation de différents types de filtres et de polariseurs. Des variations locales de la géométrie des éléments sur un substrat avec une métallisation sur la face arrière - ayant pour résultat des variations de phase due a la réflexion - peuvent être employées pour concevoir des réflecteurs à motifs imprimés (reflectarray antennas). En tenant compte des propriétés des deux polarisations pour de telles antennes, on peut construire des antennes à double fonction ou bifréquences, ou bien ces propriétés peuvent encore être exploitées pour la réalisation d'antennes a réflexion indirecte (folded reflector antennas) de faible épaisseur. Des exemples d'antennes sont présentées, utilisant les doubles caractéristiques de rayonnement, opérant en bi-bande et antennes à réflexion indirecte (folded reflector antennas) à faibles pertes.

Contents:

I. INTRODUCTION

For communication and sensor applications, antennas with low profile, low loss and low production cost are required. While planar antennas are optimal with respect to antenna depth and cost, they suffer from high losses, especially for narrow beamwidth [1], [2]. Arrays of horn antennas with a waveguide feed network [3] or waveguide slotted arrays [4], [5] are lower in loss, but partly narrow band and complicated in their design, and they do not readily lend themselves to low cost fabrication. Recently, some work has been reported on the fabrication of waveguide networks and antennas according to [3] using plastic injection molding and electroplating [6].
An alternative solution for printed antennas are quasi-optically fed printed antennas, i.e. printed reflector type antennas consisting of arrays of printed elements acting as fixed reflection phase shifters [8] - [17]. Different concepts for such antennas have been reported, ranging from Fresnel type antennas [9] to arrays with continuous phase adjustment using microstrip patch antennas with fixed length stubs [8], [12], patches with varying dimensions [10], [11], [13], [14], [16], [17], or even electronically tunable reflection phase angles [15]. This paper describes design and performance of a number of antennas based on the reflectarray principle with emphasis on the exploitation of the dual polarization properties of the planar structures.
The following section of this paper gives a short introduction into the basic computation method of periodic and non-periodic antenna structures. In the next section, a first offset fed antenna for a single polarization is presented, together with results of a full wave characterization of the complete antenna. In the fourth section, a dual polarization antenna with equal radiation characteristics in the two polarizations, but different feed points, is presented, and two different approaches for dual frequency reflectarray antennas will be demonstrated, while section V will deal with a combination of focussing reflectarray and polarization twisting, leading – together with a polarizing grid – to low profile folded reflector antennas. Examples for communication antennas in the frequency ranges of 28 GHz and 58/60 GHz will be presented.

II. SOME PRINCIPLES OF THE THEORETICAL CALCULATION OF THE ANTENNA STRUCTURES

The basis for the design procedure of reflectarray antennas as described in this paper is a periodic array of dipoles printed on a single dielectric substrate with backside metallization. Typically, the distance between the printed elements is chosen to about half a free space wavelength. In this way, grating lobes can be avoided for all antenna arrangements. The reflection behavior of such dipole arrays is calculated using a standard spectral domain method and Floquet's theorem, e.g. [7], [25]. The basic equation describing the fields excited by an incident plane wave on a periodic structure is given by

(1) $$\tilde{\vec{E}}_{total} = \tilde{\vec{\vec{Z}}} \cdot \tilde{\vec{J}} + \tilde{\vec{E}}_{in} + \tilde{\vec{E}}_{refl} \, .$$

All quantities are Fourier transforms, indicated by the tilde. The electric fields are taken in the metallization plane. $\tilde{\vec{\vec{Z}}}$ is the dyadic Green's function of a dielectric layer on a ground plane

(2) $$\tilde{\vec{\vec{Z}}} = \begin{pmatrix} \tilde{Z}_{xx} & \tilde{Z}_{xz} \\ \tilde{Z}_{xz} & \tilde{Z}_{zz} \end{pmatrix}$$ with

(3) $$\tilde{Z}_{xx} = -\frac{\alpha^2 Z_e + \beta^2 Z_h}{\alpha^2 + \beta^2},\quad \tilde{Z}_{zz} = -\frac{\beta^2 Z_e + \alpha^2 Z_h}{\alpha^2 + \beta^2},\quad \tilde{Z}_{xz} = -\frac{\alpha\beta(Z_e - Z_h)}{\alpha^2 + \beta^2},$$

(4) $$Z_e = \frac{1}{\frac{j\omega\varepsilon_0\varepsilon_r}{\gamma_2} coth(\gamma_2 h) + \frac{j\omega\varepsilon_0}{\gamma_1}},\quad Z_h = \frac{1}{\frac{\gamma_2}{j\omega\mu_0} coth(\gamma_2 h) + \frac{\gamma_1}{j\omega\mu_0}}$$

and

(5) $$\gamma_i = \sqrt{\alpha^2 + \beta^2 - k_0^2 \cdot \varepsilon_{ri}}.$$

α and β are the Fourier variables for x and z. $\vec{\tilde{J}}$ represents the current density on the strip, $\vec{\tilde{E}}_{in}$ is the incident plane wave, and $\vec{\tilde{E}}_{refl}$ is the electric field reflected by the dielectric layer ***without*** the dipoles. The indices 1 and 2 in the preceding equations refer to the free space and the dielectric layer, respectively. The current densities on the metal elements – in this paper, only rectangular elements are considered – are expanded with entire domain functions including edge terms [25]. Galerkin's method is used to transform equ. (1) into an inhomogeneous system of equations. Due to the periodic nature of this arrangement, only discrete Fourier variables have to be taken into account for the numerical procedure. The system of equation can be solved for the amplitudes of the current density functions and the reflection coefficient of the wave. The wave incident on the substrate is completely reflected, the phase angle, however, depends on dipole length and, to a minor degree only, on dipole width. In Fig. 1, the reflection phase angle is plotted for a plane wave incident from broadside. Duroid material with a thickness of 0.254 mm and a dielectric constant of 2.22 is used as substrate in this example. Frequency is 58 GHz, and element distance is 2.4 mm in both directions. The resulting phase angle varies over nearly 360°.

In a first approach, these reflection phase angles calculated from a ***periodic*** structure can be used for the design of reflectarray antennas consisting of dipoles on a periodic grid, but with varying dipole dimensions. This design procedure mostly gives reasonably good results, although it provides only a rough estimate of the actual situation. Therefore, equ. (1) was extended to the calculation of a complete reflectarray [18]. The incident field now is the field transformed from the aperture of the feeding antenna into the plane of the dipole elements. The current density now is the superposition of the contributions of all individual dipoles. Although the basic procedure remains the same as with the solution of equ. (1), there are some important differences:

§ Due to the non-periodic arrangement, the Fourier variables are continuous now. Consequently, the poles occurring in the Green's function {equs. (3), (4)} have to be taken into account by residuum calculations.

§ Due to the distances between the different dipoles, highly oscillating terms appear in the reaction integrals resulting from Galerkin's method. With a modified integration procedure including an analytical integration of an approximated kernel of the integrals, these can be evaluated effectively [19].

From the amplitudes of the current densities, both the radiation diagram of the complete antenna as well as amplitude and phase of the outgoing (plane) wave can be computed. The phase distribution of the outgoing wave calculated immediately in front of the reflectarray allows an association of phase errors to the underlying dipoles, thus enabling an optimization of the antenna.

III. OFFSET-FED PRINTED REFLECTARRAY ANTENNA

Based on earlier work [13], an offset-fed printed reflector antenna for a single polarization at 24 GHz was designed, fabricated and tested. The layout of the reflector is shown in Fig. 2. Polarization is horizontal, the diameter of the array was chosen to 200 mm, and the feed point is located 150 mm away from the substrate plane and shifted down from the array center by 216 mm. The substrate material has a thickness of 0.76 mm and a dielectric constant of 2.5. The dipoles are 1.5 mm wide. For each dipole, its length was chosen to give a plane wave front of the reflected wave propagating perpendicular to the substrate surface. The spectral domain calculation as described above was applied to the complete antenna in order to check the simple design approach.
Theoretical and experimental radiation diagrams of the offset-fed antenna for H- and E-plane are plotted in Fig. 3. Up to ±15°, the agreement is rather good; for larger angles, effects like the finite substrate size not included in the calculations or direct feed radiation lead to some deviations of the theoretical results from the measured ones.

IV. DUAL POLARIZATION ANTENNAS

As was shown in Fig. 1, the reflection phase angles of the dipoles mainly depend on length. The reflection phase angles in the orthogonal polarization then are determined by the element width. Including some minor corrections of the element geometry, reflectarray thus can be designed for mostly independent performance in the two polarizations. This may include

- equal radiation characteristics with different feed points,
- different radiation characteristics with equal or different feed points,
- operation at different frequencies,
- generation of circular polarization (to this end, a 90° phase difference has to be adjusted between the two beams with equal amplitude performance),
- generation of polarization twisting between incident and reflected wave. This will be explained and exploited in detail in section V.

As a first example to evaluate this principle, an antenna is presented having two different offset feed point, but equal radiation characteristics in the two polarizations. Such an arrangement allows an easy separation of orthogonal polarizations without the need for a separate transmission line polarizer. The antenna structure and the layout of the reflectarray are shown in detail in Fig. 4, frequency of operation is 20 GHz. The four radiation diagrams are plotted in Fig. 5. The antenna diameter of 180 mm results in nearly equal beamwidths of 5° - 5.5° for both planes and polarizations. Sidelobe level is -17 dB or better, some unsymmetry is caused by the offset feeding in both planes.

In some applications, a single aperture is required for different applications, e.g. at different frequencies. To this end, two approaches were investigated based on reflectarrays as described before. The first approach simply uses a single polarization antenna as described in section III or in [13]. As the backside metallization needs to reflect only the respective polarization of operation of the antenna, it equally can be replaced by a printed grid (Fig. 6). Together with relatively narrow dipoles, this reflectarray is nearly transparent at the orthogonal polarization. In the example presented here, the dipole width is 0.5 mm. To compensate a slight difference between the reflection phase angle of the grid and a solid metallization, the value of the thickness of the dielectric substrate is slightly modified for the design process. The focal length of this (nearly) centrally fed array is 55 mm only. Consequently, the design approach on the basis of a plane wave incident on a periodic

structure gives only a first approximation of the necessary dipole geometries. The full-wave computation method therefore was used to optimize the phase distribution in the antenna aperture.
Theoretical and experimental radiation diagrams of the antenna as depicted in Fig. 6 are plotted in Fig. 7. Although some effort was made to approximately include the blocking effect of the feed waveguide in the computation, some deviation in the side lobe level can be recognized between experiment and calculated results. Beamwidth and side lobe level are 4° and about -23 dB in the H-plane and 3.6° and -19 dB in the E-plane, respectively. The transparency of this antenna in the orthogonal polarization was tested in X-band (8 – 12 GHz), and an insertion loss of 0.2 dB only was found. As a consequence, such an antenna provides a high degree of freedom for a combination of different antenna applications in a common aperture.

In the second example, the planar reflectarray is designed for operation at two different frequencies in the two linear polarizations. To evaluate the limit of this procedure, a combination of 24 GHz and 60 GHz in a common aperture was investigated. The full range reflection angles requires a maximum dipole length of $\lambda/2$ at 24 GHz, including the effect of the dielectric. On the other hand, to avoid grating lobes at 60 GHz, the element spacing must not exceed half a free space wavelength at 60 GHz. To fulfill these two requirements, a substrate with a dielectric constant of 6 and a non-quadratic grid were chosen. Substrate thickness is 0.254 mm. The overall reflector with a diameter of 150 mm includes more than 5000 dipoles. The reflector dipole structure is shown in Fig. 8. The 24 GHz operation is performed with horizontal, the 60 GHz operation with vertical polarization. A single offset feed position was selected with a distance of 160 mm to the substrate plane and 95 mm below the array axis. Fig. 9 displays the azimuth radiation diagrams at the two frequencies. At 24 GHz, a reasonably good radiation characteristic with a beamwidth of 5.2° can be seen. At 60 GHz, shoulders at the sides of the main lobe rise up to about -15 dB, the beamwidth is 2.3°. Partly, this is due to the fact that the antenna was tested at a distance of 6 m only, compared to a necessary far field distance of 9 m according to the familiar $2D^2/\lambda$ formula.

V. FOLDED REFLECTOR ANTENNAS

The focussing array can be modified to include a polarization twisting of the electromagnetic field. Together with a printed polarizing grid or a slot array this can be applied to the design of a folded reflector antenna [20]. The principal function of this antenna arrangement is indicated in Fig. 10. The radiation of the feed is reflected by a printed grid or slot array at the front of the antenna. Then the wave is incident on the printed focussing and twisting reflector. The twisting principle of the reflector is indicated in Fig. 11. The dipole axes are tilted by 45° with respect to the incident electric field. The dimensions of the dipoles are selected in such a way that a phase difference of 180° occurs between the two components of the reflected wave. Thus, the polarization of the total reflected wave is twisted by 90° compared to the incident one. Such a twisting performance is possible for a wide variety of combinations of dipole width and length, differing only in the absolute reflection phase angle. This overall phase shift is adjusted according to the focussing (phase shifting) requirements of the reflector. The outgoing plane wave then can pass the grid or slot array (Fig. 10). The original design of this antenna once again is done on the basis of *periodic* structures. For varying dipole dimensions, the reflection phase angles are calculated for both principal polarizations. The optimum combination of phases then is selected from this set of data according to both twisting and focussing requirements.

Even circular polarization can be achieved with this type of antenna if the polarizing grid or slot array is replaced by a circular polarizer as described in [21].

Due to the folding of the printed reflector antenna, very compact, i.e. relatively low profile antennas can be realized. From the feed, the power is distributed by radiation, and most of the dipoles of the reflectarray are not in resonance. Consequently, losses are very low. As the antenna consists of two printed substrates only - together with the feed, it lends itself to a low cost design as well. In a final stage, even the feed might be integrated with the reflectarray substrate.

After first tests at 20 GHz [20], antennas of this type have been realized at 28.5 GHz, in the 60 GHz range [23], [24], and at 76.5 GHz for automotive applications, including even beam scanning by tilting the reflectarray [22] .

Fig. 12 shows the layout of the 28.5 GHz antenna designed for a point-to-point communication system. Substrate thickness for the reflector and the polarizing grid are 0.5 mm and 3.28 mm, respectively, the dielectric constant is 2.35. The distance between the two substrates is 55 mm, the size of the antenna 260 mm $\times$ 280 mm. A conical horn is used as feed. H- and E-plane radiation diagrams are plotted in Fig. 13, top. Beamwidths are 2.4° and 2.3°, and the side lobe level is better than -20 dB. At the bottom of Fig. 13, the E-plane radiation diagrams are shown at frequencies of 27.5 GHz and 29.5 GHz compared to 28.5 GHz. Except for a slight widening of the beam at a level below -10 dB, good performance can be stated over a bandwidth of at least 7%.

For the 61 GHz ISM band as well as for the 58 GHz communication band, an antenna with a diameter of 100 mm and a depth of only 25 mm was designed; the layout of the reflector is plotted in Fig. 14. Substrate thickness is 0.254 mm for the reflector and 1.58 for the polarizing grid, the dielectric constants are 2.22 and 2.35, respectively. Fig. 15 shows the E- and H-plane radiation diagrams at 58.4 GHz as well as the H-plane diagrams at 59.6 GHz and 61.6 GHz compared to that at 58.4 GHz. Except for some slight shoulders at the highest frequency, side lobe level is below –24 GHz. At 61.2 GHz, the beamwidths are 4.1° in H-plane and 3.6° in E-plane; this is larger than expected from the aperture, but as the feed horn diameter was too big, an amplitude taper of –15 dB occurred at the reflector edges. Gain was measured to 33 dB, compared to 32.6 dB calculated from the usual formula $27000/(\Theta \times \Phi)$, the beamwidths Θ and Φ taken in degrees. This demonstrates the low loss performance as mentioned above. First tests even have been initiated to further reduce the depth of this antenna; first results indicate a performance with only slightly increased side lobe levels for an antenna depth of 20 mm. Further activities are directed towards a full wave characterization of this type of antenna to enable an optimization as it was done with the 35 GHz antenna (section IV, [18], [19]). In this case, however, there is a wide variation of dipole widths requiring a higher number of expansion functions for the current densities on the dipoles. This – together with the necessity to take into account two polarizations – leads to a considerably increase of computational effort. First results have been obtained for the 60 GHz antenna, although a good convergence has not really been achieved. Nevertheless, a reasonable agreements between theory and experiments can be stated with this first effort, as can be seen from Fig. 16.

VI. CONCLUSION

Design, partly optimization, and experimental results have been demonstrated for a number of reflectarray antennas. Both lengths and widths of the reflecting elements are included into a dual polarization design. This includes antennas with dual frequency operation. If the dual polarization properties are used to provide a polarization twisting operation, low profile, low loss, and potentially, low cost mm-wave antennas can be realized. Practical examples have been demonstrated at 28.5 GHz and 60 GHz. Shortly, some effort have been described to do a full wave calculation of these reflectarrays; this ongoing effort probably will allow to optimize these antennas and to further reduce their depth.

REFERENCES

[1] RUSSELL (M. E.) et al., Millimeter-wave radar sensor for automotive intelligent cruise control (ICC). IEEE Trans. Microw. Theor. Techniques MTT-45 (1997), pp. 2444 - 2453.

[2] MANSEN (D.), VILLINO (G.), Planar Microstrip Antennas for MMDS Application at 40GHz. 28th European Microw. Conf. 1999, Munich, Germany, Vol. III, pp. 9 - 12.

[3] SEHM (T.), LEHTO (A.), A. V. RÄISÄNEN (A. V.), A high-gain 58 GHz box-horn array antenna with suppressed grating lobes. IEEE Transactions on Antennas and Propagation, Vol. 47, No. 7, 1999, pp. 1125–1130.

[4] ANDERSON (T. N.), MICHALSKI (J.), HOU (Yun-Li), A high power, high performance planar slot array antenna. Microw. Journal, May 1995, pp. 70 – 77.

[5] ANDO (M.) et al., Novel single-layer waveguides for high-efficiency millimeter-wave arrays. IEEE Trans. on Microw. Theory Tech., MTT-46 (June 1998), pp. 792 – 799.

[6] DOLP (R.), MAYER (W.), GRABHERR (W.), 58GHz High Gain Flat Panel Antenna for High Volume Production. 28th European Microw. Conf. 1999, Munich, Germany, Vol. III, pp. 12 -15.

[7] MITTRA (R.) et al., Techniques for analyzing frequency selective surfaces - a review. Proceedings of the IEEE, 76 (12), pp. 1593 - 1615, Dec. 1988.

[8] MUNSON (R. E.), HADDAD (H. A.), HANLEN (J. W.), Microstrip Reflectarray for Satellite Communication and Radar Cross-Section Enhancement or Reduction. US Patent No. 4,684,952, Sept. 24, 1982.

[9] HUDER (B.), MENZEL (W.), Flat printed reflector antenna for mm-wave application. Electronics Lett. 1988, p. 318.

[10] GUO (Y. J.), BARTON (S. K.), A High-Efficiency Quarter-Wave Zone Plate Reflector. IEEE Microwave and Guided Wave Letters, vol. 2, 1992, 470-471.

[11] GUO (Y. J.), BARTON (S. K.), Fresnel Zone Plate Reflector Incorporating Rings. IEEE Microw. and Guided Wave Letters, vol. 3, 1993, 417-419.

[12] JAVOR (R. D.), WU (X.-D.), CHANG (K.), Design and performance of a microstrip flat reflectarray antenna. Microwave And Optical Technology Letters, Vol. 7, No. 7, May 1994, pp. 322 – 324.

[13] MENZEL (W.), A planar reflector antenna. MIOP 1995, Sindelfingen, Germany, pp. 608 - 612.

[14] POZAR (D. M.), TARGONSKI (S. D.), SYRIGOS (H. D.), Design of millimeter wave microstrip reflectarrays. IEEE Trans. on Antennas and Propagation, Vol. AP-45 (1997), pp. 287 – 296.

[15] PATEL (M.), THRAVES (J.), Design and development of a low cost, electronically steerable, X-band reflectarray using planar dipoles. Military Microwaves, 1994, pp. 174 – 178.

[16] BRADLEY (J.), CUHACI (M.), SHAKER (J.), JETTÉ (S.), PETOSA (A.), A novel bifocal dual-frequency, dual orthogonal polarization planar reflector for SatCom applications. AP2000, Davos, April 2000, Session 5A2 (paper 0774).

[17] ENCINAR (J. A.), ZORNOZA (J. A.), Design and Development of Multilayer Printed Reflectarrays for Dual Polarisation and Bandwidth Enhancement, AP2000, Davos, April 2000, Session 4A9 (paper 0236).

[18] PILZ (D.), MENZEL (W.), Full Wave Analysis of a Planar Reflector Antenna. 1997 Asia Pacific Microwave Conf. APMC'97, Dec. 2 - 5, 1997, Hong Kong, pp. 225 – 227.
[19] PILZ (D.), MENZEL (W.), A mixed integration method for the evaluation of the reaction integrals using the spectral domain method. IEE Proc. on Microwaves, Antennas and Propagation, Vol. 146, No. 3, June 1999, pp. 214 – 218.
[20] PILZ (D.), MENZEL (W.), Folded reflectarray antenna. Electron. Lett., Vol. 34, No. 9, April 1998, pp. 832–833.
[21] PILZ (D.), MENZEL (W.), A novel linear-circular polarization converter. 28th Europ. Microw. Conf., 1998, Amsterdam, Vol. 2, pp. 18 – 23.
[22] MENZEL (W.), PILZ (D.), LEBERER (R.), A 77 GHz FM/CW radar front-end with a low-profile, low-loss printed antenna. IEEE Trans. on Microw. Theory Tech., Vol. MTT-47, No. 12 (Dec. 1999), pp. 2237 – 2241.
[23] MENZEL (W.), PILZ (D.), Printed quasi-optical mm-wave antennas. Millenium Conf. on Antennas and Propagation AP2000, Davos, Switzerland, 2000, Session 3A2-1 (paper no. 0023).
[24] MENZEL (W.), PILZ (D.), Printed mm-wave folded reflector antennas with high gain, low loss, and low profile. IEEE Antennas and Propagation Conf. 2000, Salt Lake City, USA, July 2000, paper 42P6.
[25] ITOH (T.) (editor), Numerical Techniques For Microwave And Millimeter-Wave Passive Structures. John Wiley & Sons, 1989.

BIOGRAPHIES

Dietmar PILZ received his Dipl.-Ing. degree from the University of Ulm, Germany, in 1994, and the Dr.-Ing. degree from the University of Ulm, Germany, in 1999. From 1994 to 1999, he worked in the Microwave Department of the University of Ulm as research assistant and PhD student. His areas of work included planar and quasi-planar structures for antenna applications. In 1999, he joined the DaimlerChrysler Aerospace in Ulm. His current areas of interest are mm-wave circuits and systems and antennas.

Wolfgang MENZEL received his Dipl.-Ing. degree at the Technical University of Aachen, Germany, in 1974, the Dr.-Ing. degree from the University of Duisburg, Germany, in 1977. From 1979 to 1989, he worked in the mm-wave department of AEG in Ulm (now DaimlerChrysler Aerospace). From 1980 to 1985, he was head of the laboratory for integrated mm-wave circuits, from 1985 to 1989 head of the mm-wave department. In that time, his areas of work included planar antennas, planar integrated circuits and system in the mm-wave frequency range. In 1989, he got a full professorship at the University of Ulm. His current areas of interest are (multi-layer) planar and waveguide circuits, antennas, mm-wave interconnects and packaging, and mm-wave system aspects.

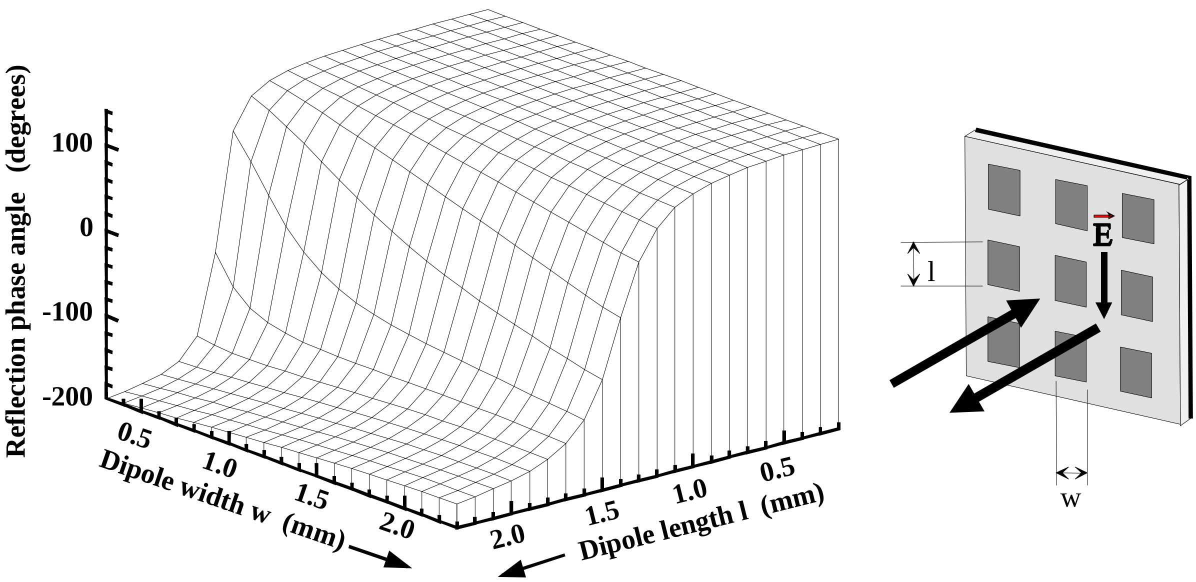

FIG. 1 — Reflection phase angle of a plane wave reflected from a periodic array of printed dipoles. (Frequency 58 GHz, substrate thickness 0.254 mm, dielectric constant 2.22, dipole grid spacing 2.4 mm, normal incidence of the wave).

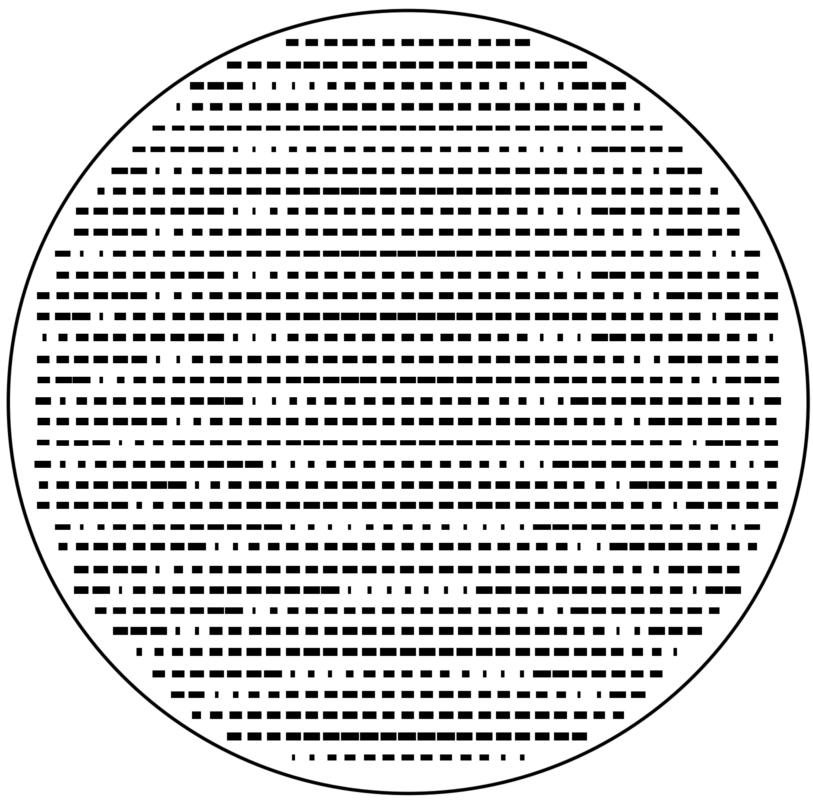

FIG. 2 — Layout of the 24 GHz, single polarization printed offset reflectarray.

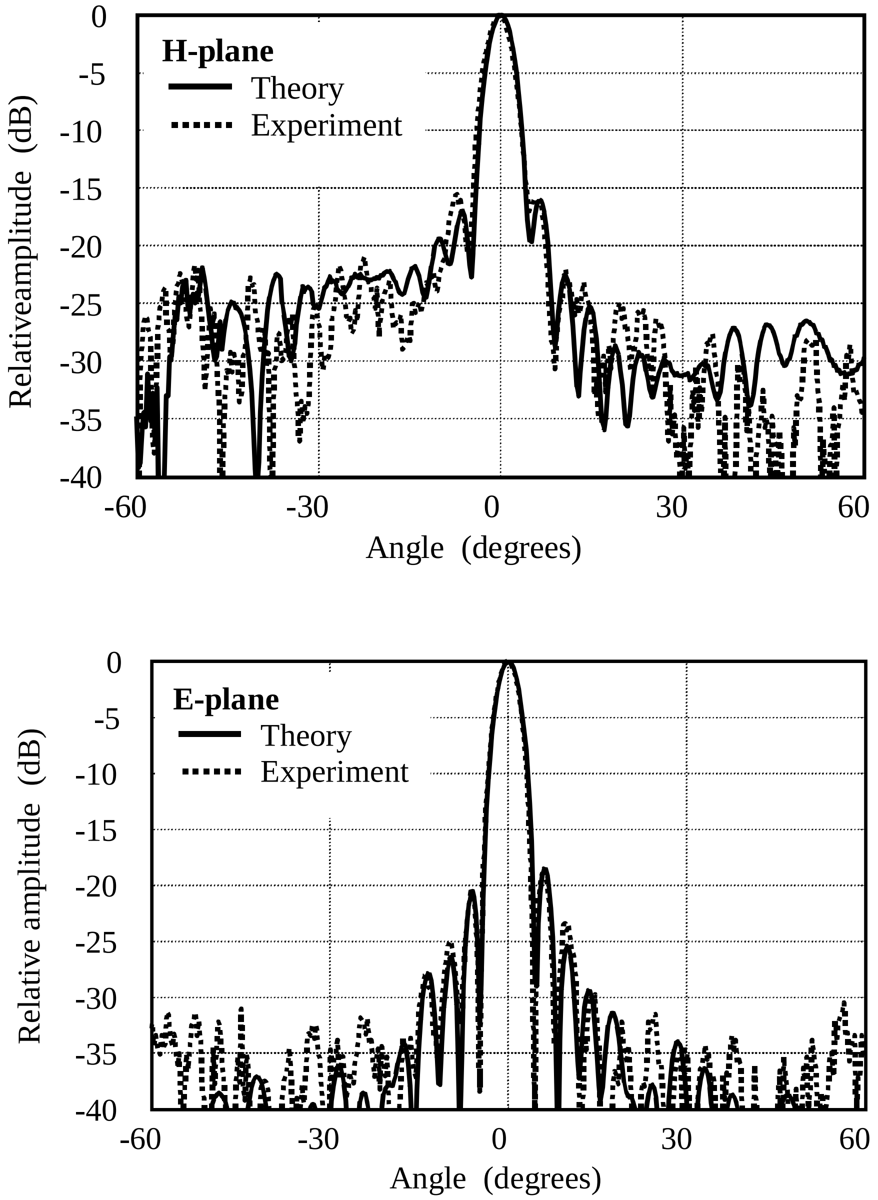

FIG. 3 — Calculated and measured H- and E-plane radiation diagram of the offset-fed printed reflectarray antenna. (Substrate thickness 0.76 mm, dielectric constant 2.5, frequency 24 GHz).

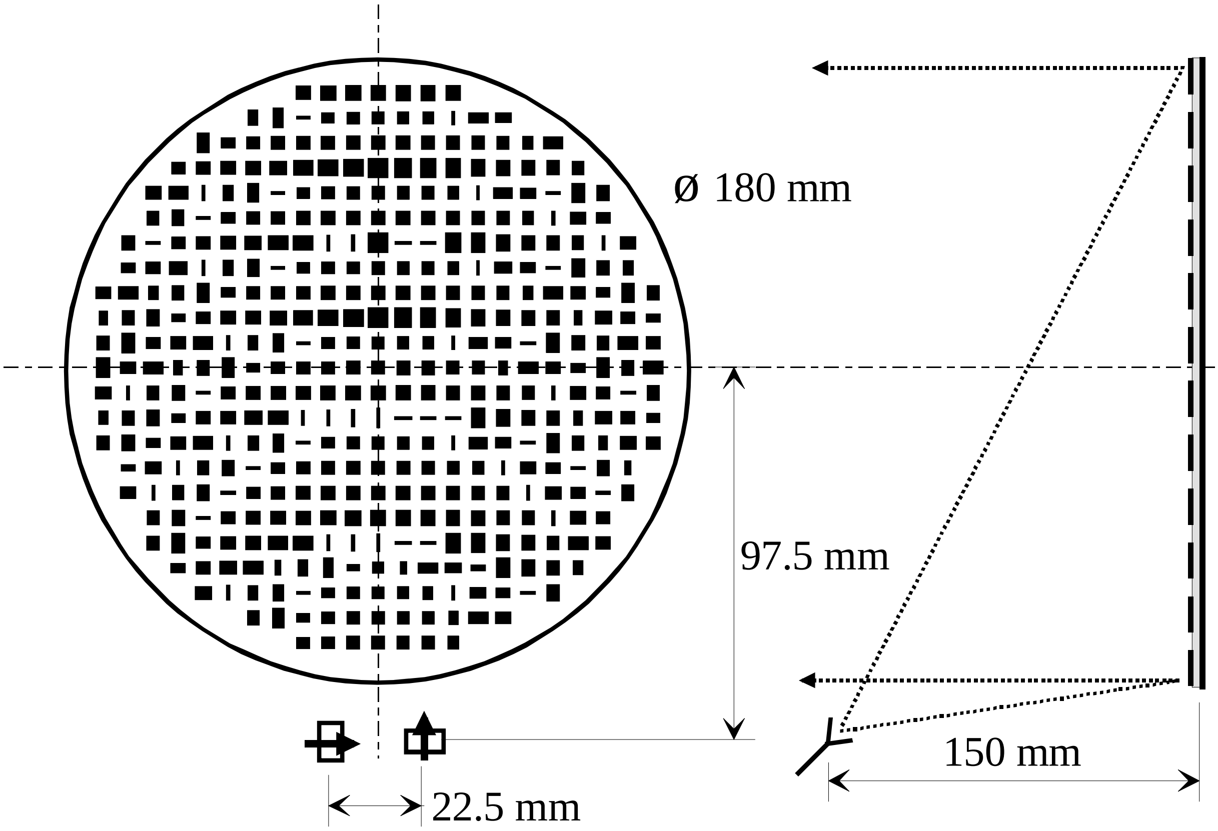

FIG. 4 — Layout and structure of the 20 GHz dual polarization reflectarray antenna with two different feed points.

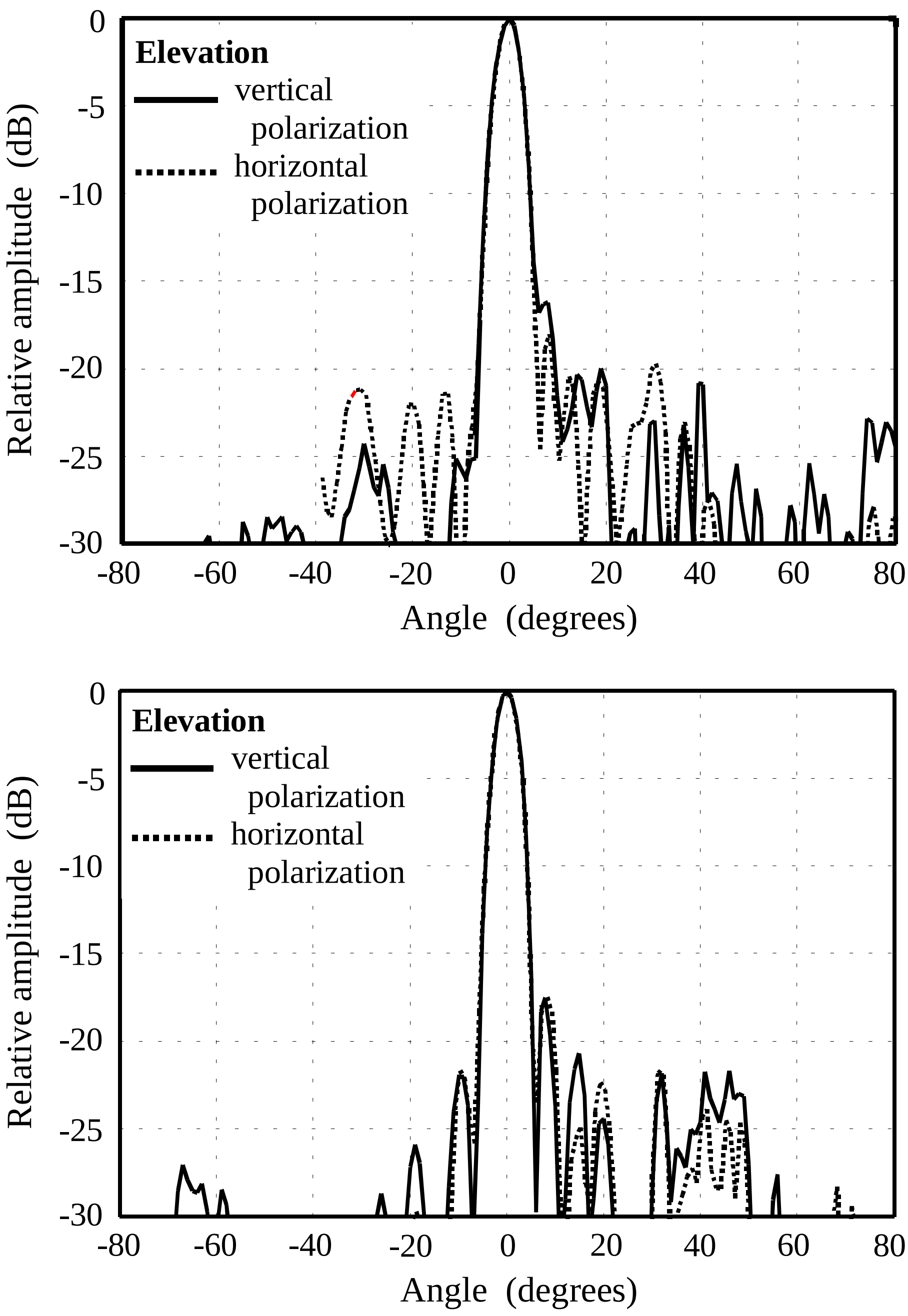

FIG. 5 — Radiation diagrams of dual a polarization reflectarray for two different feed points. (Substrate thickness 0.76 mm, dielectric constant 2.5, cell size 7.5 mm × 7.5 mm, frequency 20 GHz).

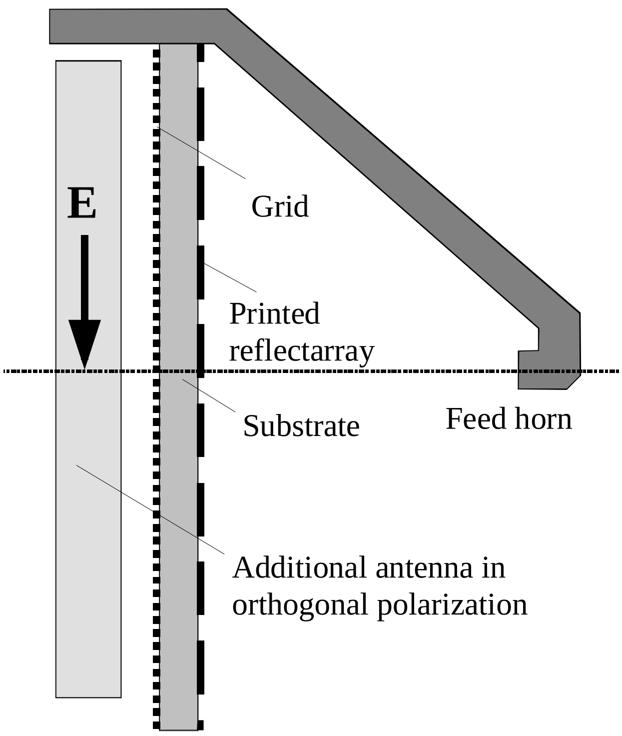

FIG. 6 — Basic principle of a "transparent" antenna using a printed reflectarray with a grid as ground plane.

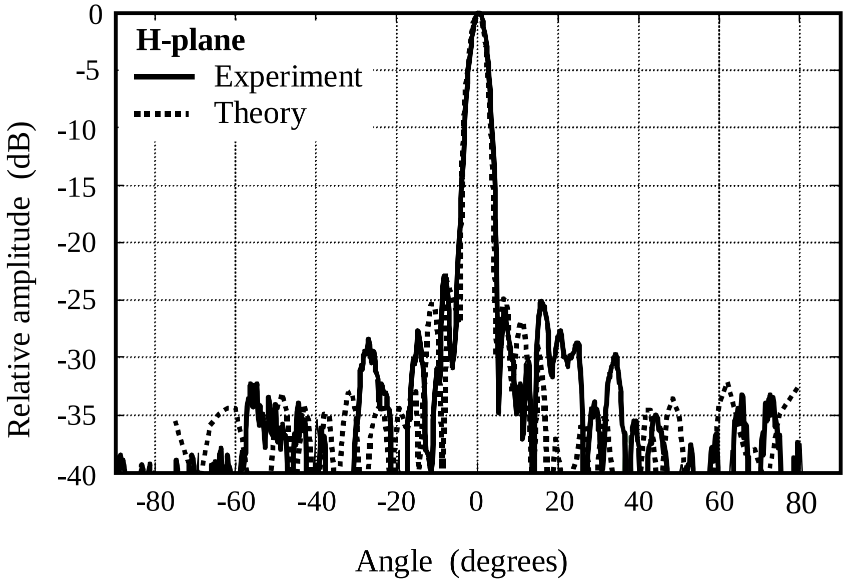

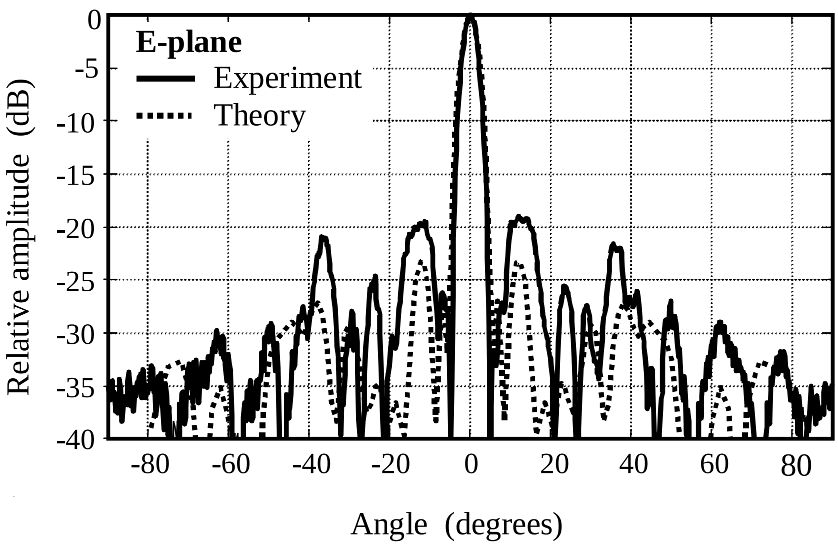

FIG. 7 — Radiation characteristics of the "transparent" reflectarray (Substrate thickness 0.76 mm, dielectric constant 2.5, cell size 5 mm × 5 mm, frequency 35 GHz).

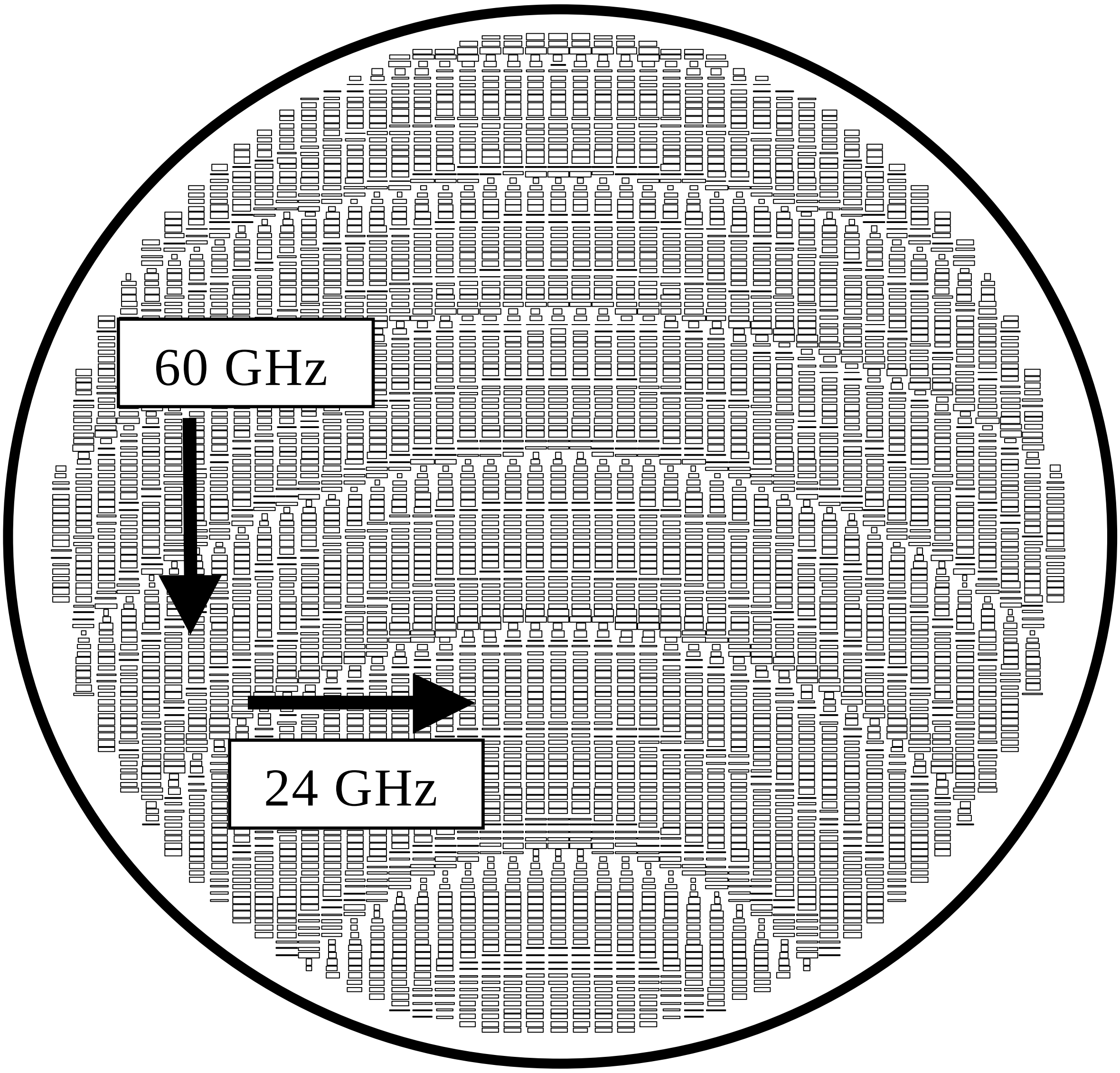

FIG. 8 — Layout of a 24/60 GHz dual frequency reflectarray antenna.

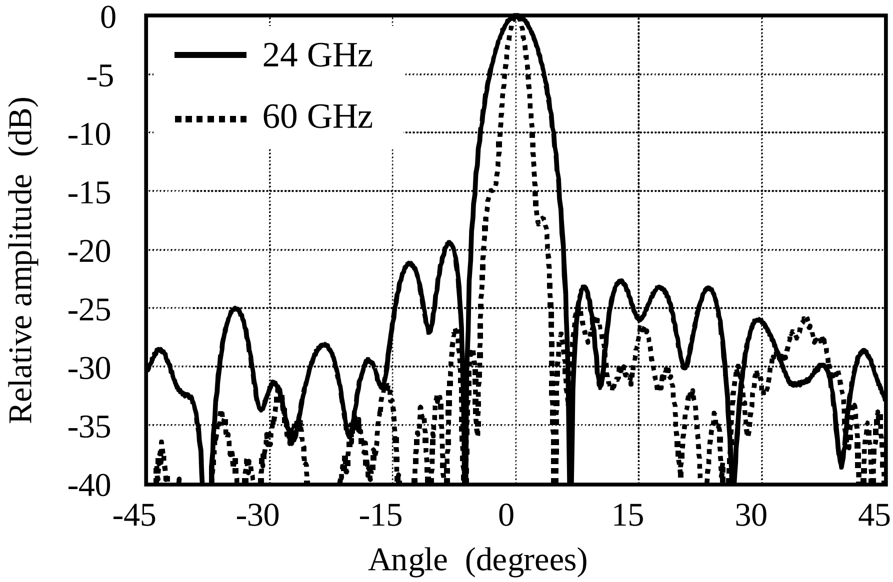

FIG. 9 — Azimuth radiation diagrams of the dual frequency reflectarray antenna. (Substrate thickness 0.254 mm, dielectric constant 6, cell size 3 mm × 1 mm).

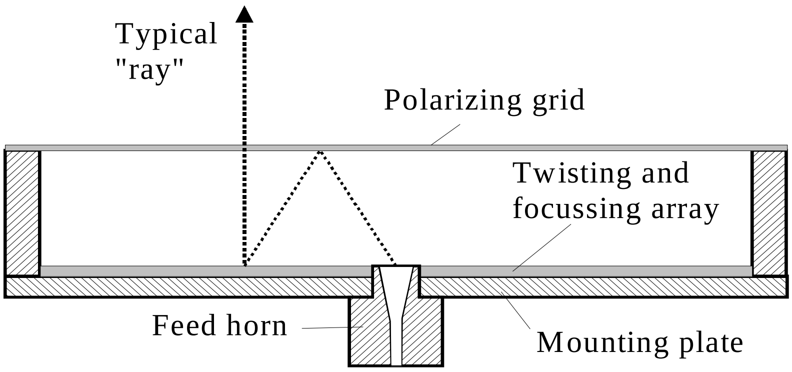

FIG. 10 — Principal setup of a printed folded reflector antenna.

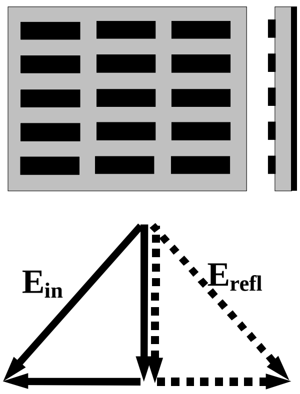

FIG. 11 — Principle of polarization twisting by a printed periodic reflectarray.

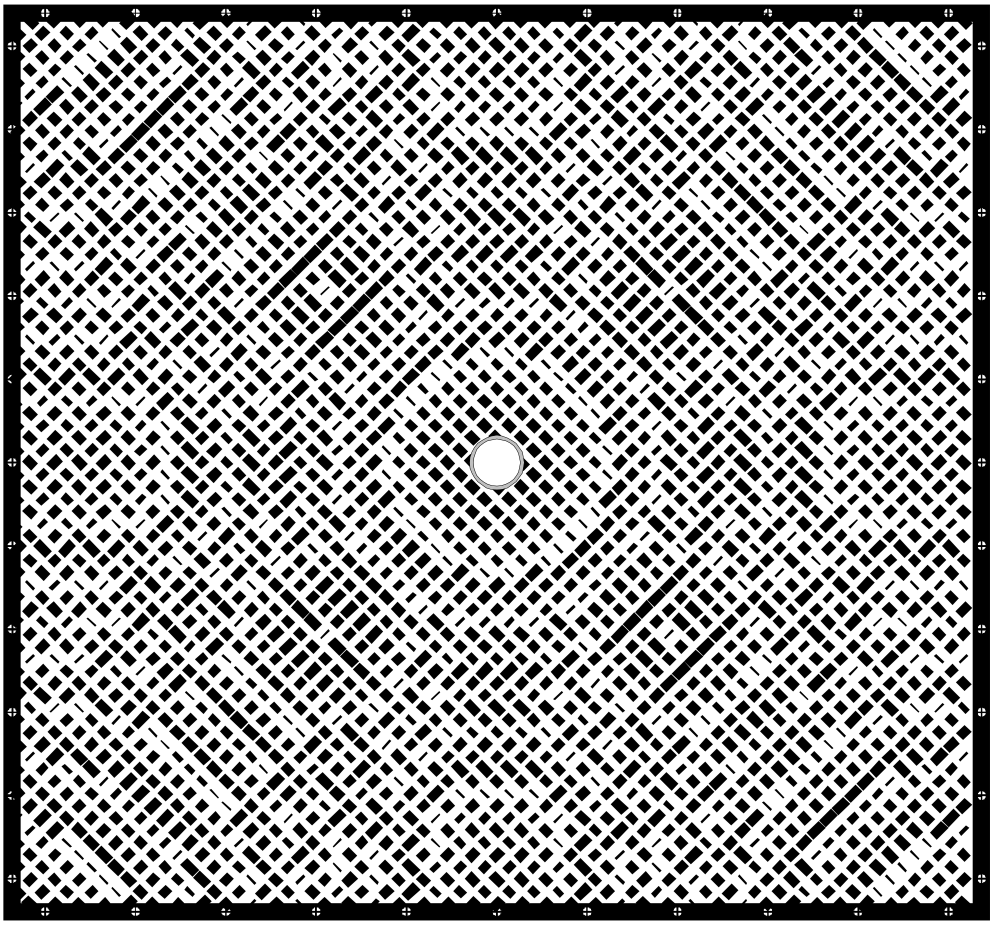

FIG. 12 — Layout of the focussing and twisting reflector for the 28 GHz reflectarray antenna.

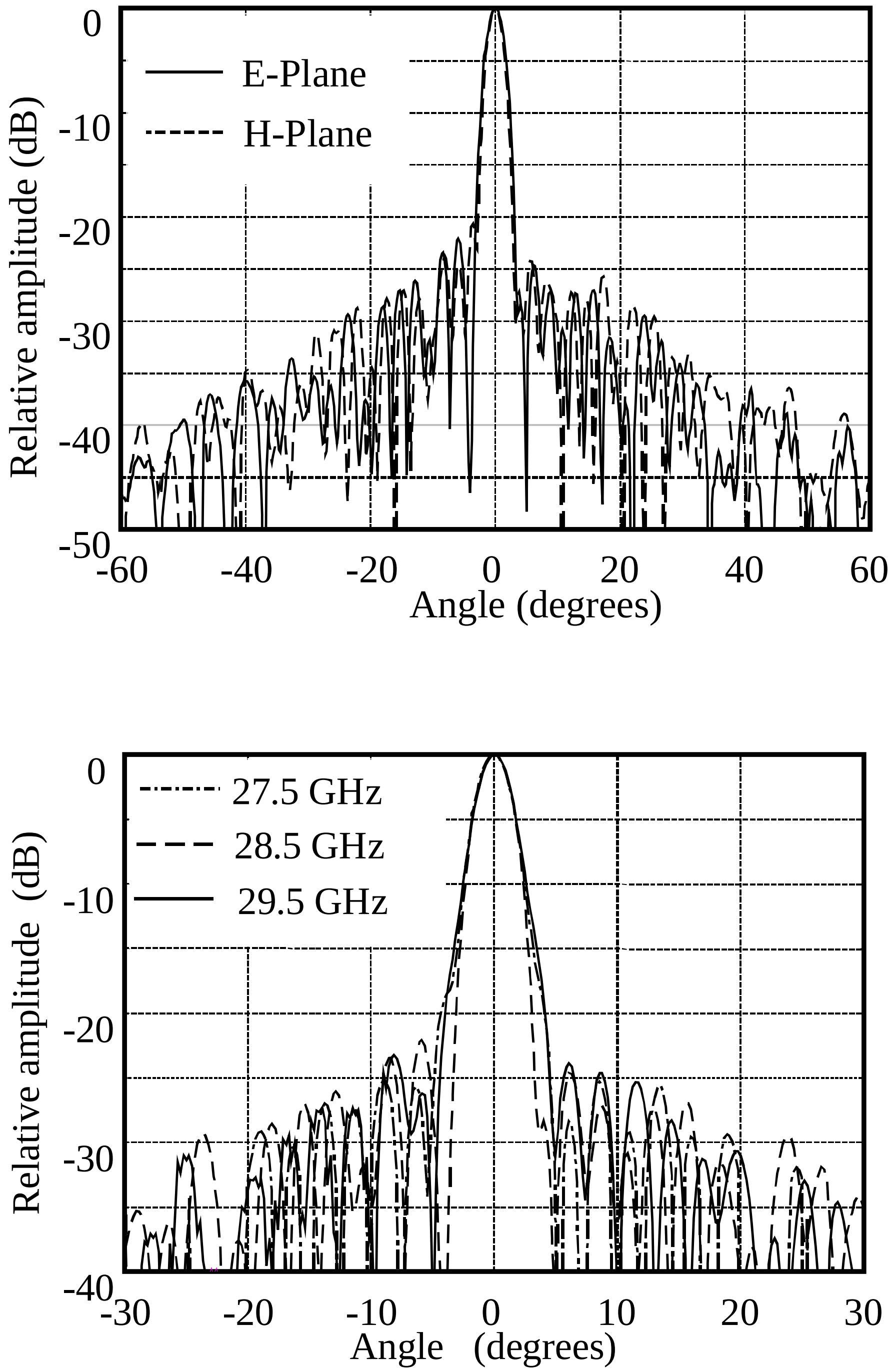

FIG. 13 — Radiation diagrams of the Ka-band folded reflector antenna. (Top: E- and H-plane at 28.5 GHz. Bottom: E-plane at 27.5 GHz, 28.5 GHz, and 29.5 GHz. Reflector: substrate thickness 0.5 mm, dielectric constant 2.22, cell size 4.8 mm × 4.8 mm. Grid: substrate thickness 3.28 mm, dielectric constant 2.35).

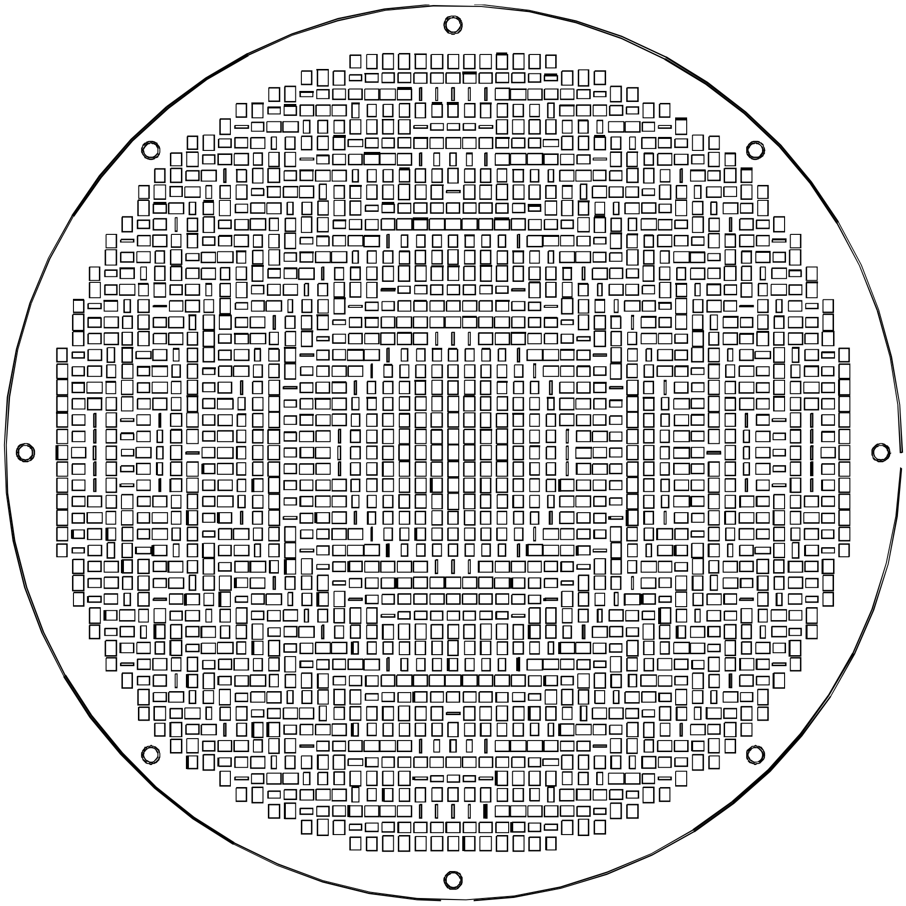

FIG. 14 — Layout of the 58/60 GHz folded reflectarray antenna.

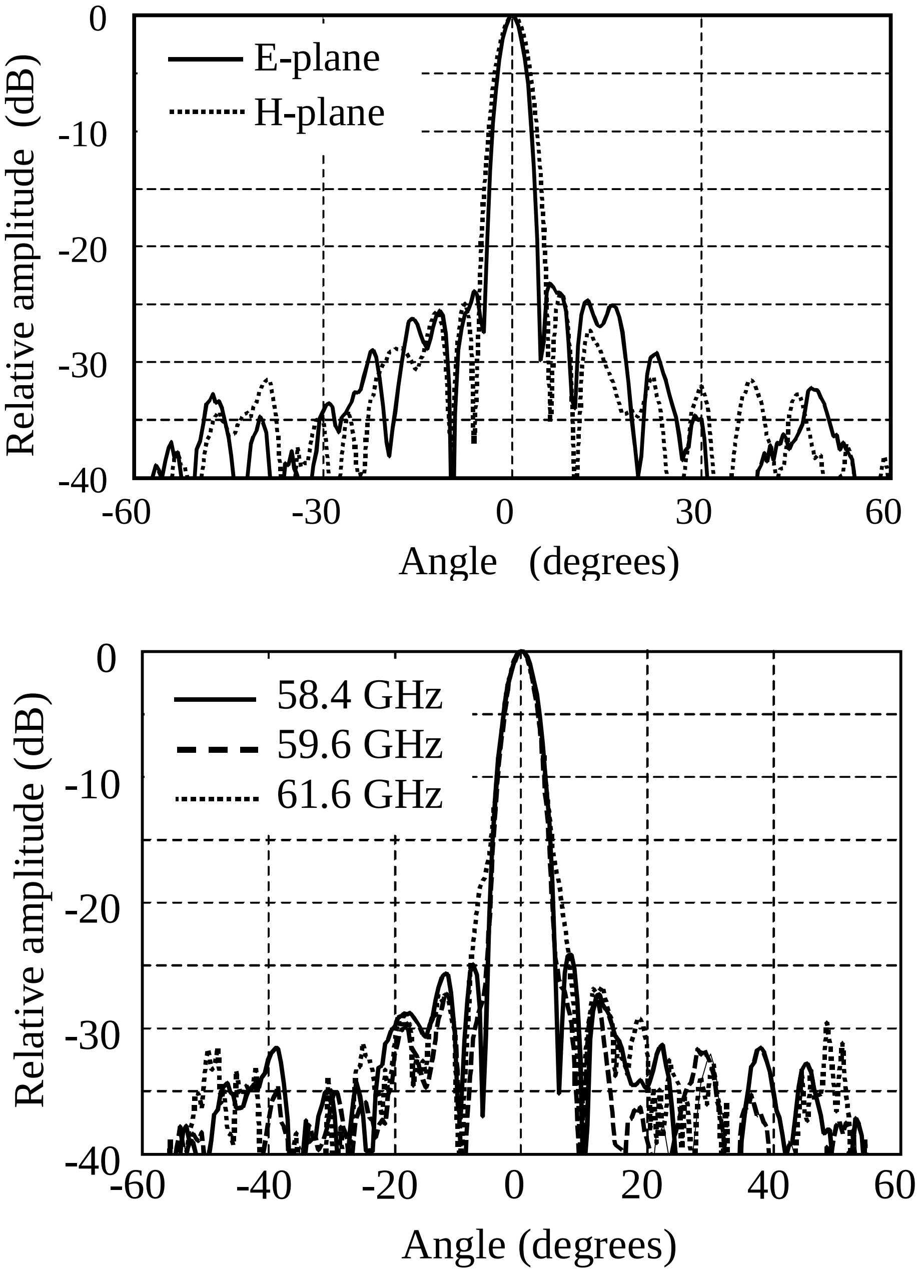

FIG. 15 — Radiation diagrams of the V-band folded reflector antenna. (Top: E- and H-plane at 58.4 GHz. Bottom: H-plane at 58.4, 59.6, and 61.6 GHz. Reflector: substrate thickness 0.254 mm, dielectric constant 2.22, cell size 2.4 mm × 2.4 mm. Grid: substrate thickness 1.58 mm, dielectric constant 2.35).

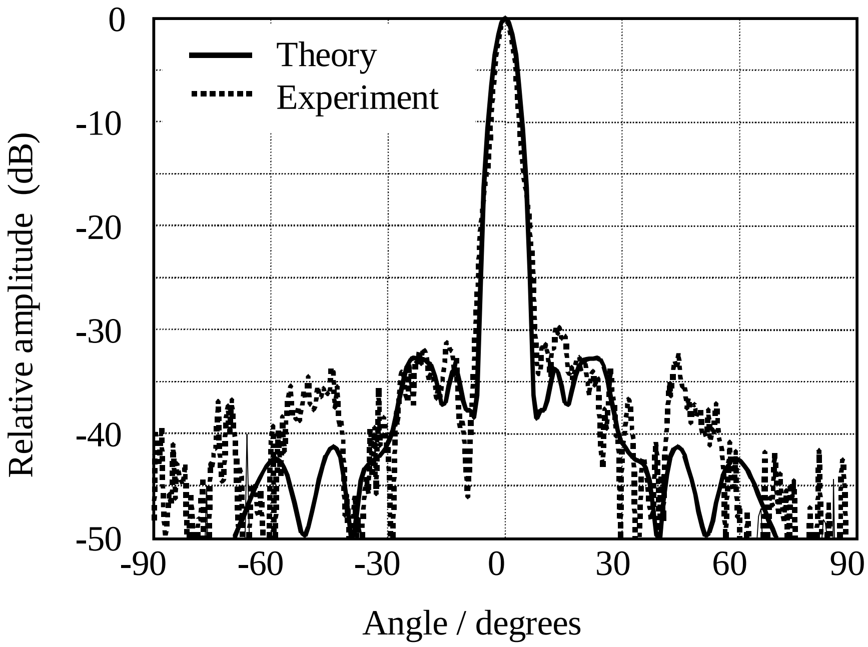

FIG. 16 — Theoretical and experimental E-plane radiation diagrams of the V-band folded reflector antenna at 61.2 GHz. (Data see FIG. 15).